

Article

Lubricity Assessment, Wear and Friction of CNT-Based Structures in Nanoscale

Elias P. Koumoulos and Costas A. Charitidis *

Research Unit of Advanced, Composite, Nano-Materials and Nanotechnology, School of Chemical Engineering, National Technical University of Athens, Athens 15780, Greece; elikoum@chemeng.ntua.gr

* Correspondence: charitidis@chemeng.ntua.gr; Tel.: +30-210-772-4046

Academic Editor: James E. Krzanowski

Received: 4 May 2017; Accepted: 13 June 2017; Published: 16 June 2017

Abstract: In this work, three case studies are reported, namely carbon nanotube/polyvinyl butyral composites, MWCNTs/polydimethylsiloxane-based coatings and vertically aligned CNT forest array, of which the friction and resistance to wear/deformation were assessed through nanoindentation/nanoscratch. Additional deformation parameters and findings are also addressed and discussed; namely, material deformation upwards (pile-up) or downwards (sink-in) with respect to the indented surface plane, hardness to modulus ratio (index of resistance to wear) and coefficient of friction. The enhancement of the scratch resistance due to the incorporation of CNTs in a polymer matrix is investigated. For the case of the forest structure, sliding between neighboring nanotubes is identified, while, through ploughing of the tip, local deformation and the extent of plasticity are also addressed.

Keywords: carbon nanotubes; composites; nanoscratch; coefficient of friction; nanoindentation; carbon

1. Introduction

Composites with (also carbon-based) nanofillers form a promising new group of materials which align the advantages of both the matrix (polymer mostly) and filling material, with the prerequisite of strong interfacial bonding [1]. Carbon nanotubes (CNTs), exhibiting increased mechanical and electrical properties, high aspect ratio and low density, have been extensively investigated in order to improve the polymer matrix characteristics [2]. One of the key aspects, when CNTs are used as filler in polymer matrix, is the issue of sufficient dispersion. This issue is crucial to uniformly transfer the filler properties (e.g., mechanical load) to the matrix. Numerous techniques have been applied to successfully disperse CNTs, and results denote that the entanglement of CNTs is a key yet negative issue [3]. Therefore, it is crucial to generate from a less entangled material so as to have a better dispersion of CNTs in the polymer matrix. Multi-wall CNTs (MWCNTs), having typically higher tube diameter than single-wall CNTs (SWCNTs), are in principle easier to disperse in a polymer matrix. Several similar works in literature have studied the elasticity [4,5], damage [6], buckling [7,8], tribology [9,10] and toughness [11] of CNT-filler polymer (mainly) composites.

The tribological properties of CNT-polymer composites are being assessed by using reciprocating wear and friction machine under different sliding conditions; friction force, wear loss and friction coefficient significantly increase with increase in load at fixed sliding time, while wear loss significantly decreases with increase of sliding time at certain applied load. However, sliding temperature is reported to gradually reduce and stabilize after a short period of time (5 min) [12]. Investigation of carbon nanotube reinforced epoxy composite revealed that the surface coverage area of CNTs plays a significant role in the wear of the composites. With surface coverage area of CNTs greater than 25%, the wear rate is reduced by a factor of 5.5. Improvement of the wear resistance of a high surface coverage area of CNTs was concluded to appear due to the CNTs exposed to the sliding interface

which protected the epoxy matrix effectively. Contact sliding in a wear test revealed CNT significant deformation and cause its fragmentation [13].

The layered graphite-like structure of CNTs in combination with their performance (i.e., strength, stiffness, thermal conductivity and density) make them an ideal category of materials for a wide range of engineering applications. Specifically, recent findings on the utilization of CNTs in tribology mainly for anti-friction, wear-proof and self-lubrication, address direct insertion of CNTs as additives/fillers in various lubricant media in liquid state or embedded as fillers in polymer, metal and ceramic matrices. However, critical issues such as processing technique, CNT dispersion and interfacial bonding have to be confronted, as the mechanisms should be considered with respect to the improvement in tribological performance [14].

As operating environment in many industrial applications results in the pair under tribo conditions to operate in the mixed lubrication regime; when the lubricant layer thickness is insufficient to separate the sliding, usage of lubricant with anti-wear additives is essential. To this regards, recent studies include experiments conducted on block and disk test setup to determine the effect of using CNT as anti-wear additive in a commercial lubricant (varying quantities of the CNT have been tried in the lubricant to conduct the wear tests) [15]. Three different functionalized (surface grafted carboxyl groups and amino groups) were investigated and the results indicate that compared with pure epoxy resin, MWCNTs composites exhibited decreased friction coefficient and wear rate (wear rate decreased with the increase of MWCNT concentration); to this regard, MWCNTs—epoxy composites improve the wear resistance and decrease the coefficient of friction.

The influence of CNT when combined with friction powder prepared through different process parameters on flexural properties is recently reported, in order to assess friction performance of automotive brake friction materials; the findings indicate that flexural property and friction performance are significantly affected when the modified CNT/friction powders are used. However, it is worth noting that amorphous carbon clusters and CNTs aggregation are formed when higher concentration of catalyst are used, leading to faulty specimens and decrease of reinforcement effectiveness [16,17].

In this work, three case studies are reported, namely carbon nanotube/polyvinyl butyral composites [15], MWCNTs/polydimethylsiloxane-based coatings [16] and vertically aligned CNT forest array [17], of which the friction and resistance to wear/deformation were assessed through nanoindentation/nanoscratch.

2. Experimental—Materials and Methods

Deformation during nanoscratch, resistance to wear and coefficient of friction were investigated via Hysitron TriboLab[®] Nanomechanical Test Instrument, Minneapolis-Minnesota USA (also able to perform as Scanning Probe Microscope (SPM)), with a load range from 1 to 30,000.00 μN and displacement application as a function of applied load (load resolution (1 nN), displacement resolution (0.04 nm)). In all nanoindentation tests a total of 10 indents were averaged so as to determine the mean hardness (H) and elastic modulus (E) values for statistical purposes (spacing of 50 μm), in a clean area environment with 45% humidity and 23 °C ambient temperature (operated under feedback closed loop load or displacement control). All nanoscratch measurements have been performed using the standard three-sided pyramidal Berkovich probe, with an average radius of curvature of about 100 nm [15]. Hardness and E values can be extracted from the experimental data (load-displacement curves) using the Oliver-Pharr (O&P) method, for nanoindentation procedure [16,17]. The nanoscratch experimental procedure consisted of a scratch of the surface for a time of 50 s, and then a maximum imposed load (50 μN). Preparation of the samples is reported in previous works, for the case studies of carbon nanotube/polyvinyl butyral composites [15], MWCNTs/polydimethylsiloxane-based coatings [16] and vertically aligned CNT forest array [17].

To prepare CNTs–PVB (Butvar B-98, Sigma-Aldrich, St. Louis, MO, USA) composites, PVB was dissolved in a mixture of ethanol (Carlo Erba) (two parts) and 1-butanol (Sigma-Aldrich) (three parts) solvents. The CNTs was added into the PVB solution. The uniform dispersion of CNTs in composite

solution was achieved by vigorous stirring (1200 rpm). Viscous nature of the solution entrapped the gas bubbles. Sonication (ultrasonic frequency, 37 KHz) was carried out for 10 min so as to release the entrapped bubbles in the mixture. A 20-min degassing in vacuum step was subsequently undertaken to fully get rid of the trapped solvent gas bubbles. The composite was then cured in oven at 70 °C for 4 h. Samples were prepared with four different MWCNTs contents: 0.5, 1, 3, and 5 wt %. PVBC_x where *x* is the CNTs content in wt % (i.e., PVBC3.0 is 3% sample) [15].

The studied PDMS coatings were based on PDMS (Sylgard 184, Dow Corning, Midland, MI, USA). This silicon elastomer is supplied as a two-part component; base material (Part A) and curing agent (Part B), to be mixed in a ratio 10:1 by weight. After the mixing, polymerisation via hydrosilylation occurs, and a cross-linked polymer is received as a final product. MWCNT, pristine and functionalised with carboxyl groups (MWCNT-COOH), purchased by Nanothinx S.A., Patras, Greece, were tested as possible nanofillers. Both materials had average purity of 97%, external diameter of 15–35 nm and an average length of at least 10 µm [16].

For the CNT forest, a thermal CVD reactor was used to synthesize the VA-MWCNT structure. The reactor consists of a horizontal quartz tube with 3.4 cm inner diameter and 100 cm long housed in a three-zone cylindrical furnace 80 cm long. More analytically, a pyrex flask containing the reagent mixture that composed by camphor (96% purity in weight, Sigma-Aldrich, St. Louis, MO, USA) as carbon precursor and ferrocene (98% purity in weight, Sigma-Aldrich) as catalyst compound in a 20:1 mass ratio was connected to the tube nearby the nitrogen inlet. A heater plate was located below the flask, to achieve the heating and sublimation of the reactants. Nitrogen gas flow was used to carry the gas mixture of precursors towards the center of the furnace, where pyrolysis of the gases took place at 850 °C and forests of CNTs were deposited on silicon wafers [17].

3. Results and Discussion

3.1. Carbon Nanotube/Polyvinyl Butyral Composites (PVBC)

For the carbon nanotube/polyvinyl butyral composites case, as CNT concentration is increased (PVBC5.0, where 5.0 indicated the CNT addition percentage (5%)), a large raise in the stiffness of the system is evidenced, which leads to energy dissipated reduction during the experiment; however, there is more tube–tube slip in the system at higher concentration, since percolation, coupled to sufficient dispersion leads to a higher contact surface among CNTs. The mechanical properties are reported to decrease with an increase in CNTs, after a threshold concentration, a fact that is probably attributed to extensive tube–tube slip mechanism. For concentrations above percolation threshold, particle contacts occur, due to sticky inter-particles potential; extensive agglomerate regions act as resulting mechanical defects for the composite [18–24].

In nanoscratch process, as the scratch tip ploughs through the material ahead of it, the material will be either pushed forward or piled up sideways [25]; this is usually noted for relatively ductile polymers, where ironing and plastic deformation occur. In addition to the surface friction between the substrate and the scratch tip, the material is accumulated ahead of the indenter.

Coefficient of friction (CoF) is defined as the ratio of the lateral force to the normal force, while depends on indenter geometry, surface roughness of the sample, and the material properties of the sample (homogeneity, crystallinity, orientation). Rather than simply being a friction index, CoF value is also a measure of the resistance to scratch (e.g., a harder, wear-resistant material exhibits more resistance to scratch, while the tip will consequently experience a larger lateral force). In Figure 1, CoFs for all samples are presented (four scratches under same conditions were performed at three samples of each type for reproducibility). The CoF ranges from 1 to 0.5 continuously at the beginning of scratching, which is corresponding to the loading stage (PVBC1.0 and neat PVB matrix). Then it remains unchanged at 0.5 (25 s) during the steady scratching process; the average values of this stage are taken as the effective friction coefficient. These CoF trends are rather same for both samples, implying no significant differences. For neat PVB matrix, the CoF is reduced with increasing normal

load to a minimum value (~ 0.5) and remains constant, implying that plastic flow is the dominant deformation mode. For PVBC1.0, the CoF decreases with increasing normal load to a minimum value of ~ 0.52 , which corresponds to the initiation of scratching, then increases again to finally decrease to ~ 0.48 . While the main friction mechanism in the first stage was adhesion, both adhesion and ploughing contribute to the CoF in the last stage. PVBC5.0 exhibits increased CoF, when compared with neat PVB matrix and PVBC1.0; thus, nanoscratching testing showed that there is significant improvement in the scratch resistance due to incorporation of CNTs [15].

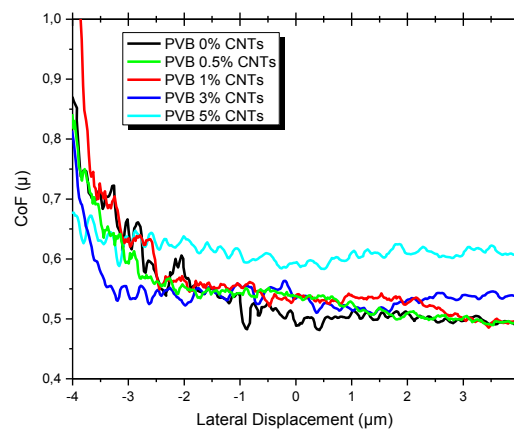
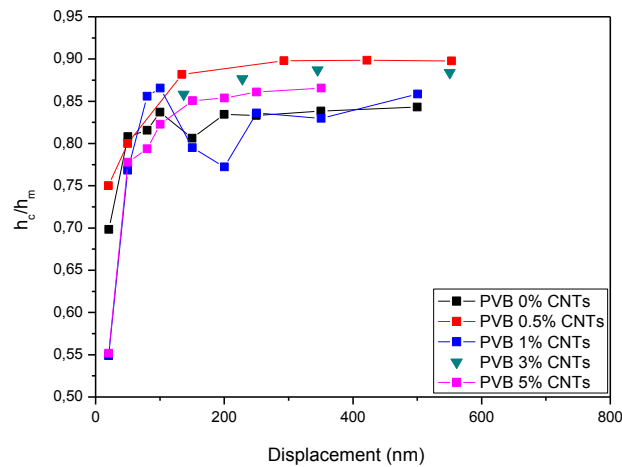


Figure 1. Coefficient of friction for PVB–CNT composites, obtained through nanoscratch testing [15].

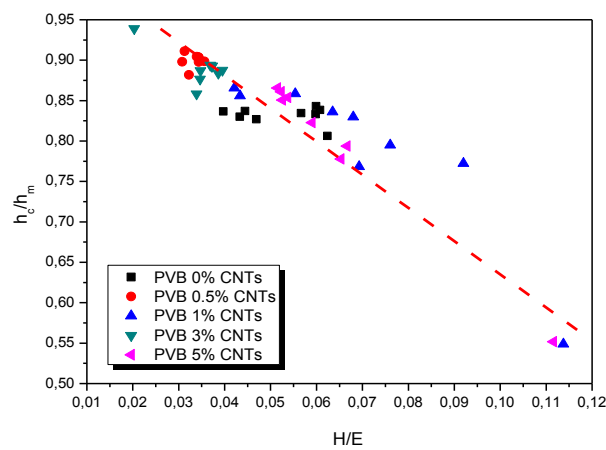
An important issue of nanoindentation measurements is that the material around the contact area tends to (plastically) deform upwards (so-called pile-up) or downwards (so-called sink-in) with respect to the indented surface region. The appearance of such piled-up and sinked-in areas is usually interpreted in terms of the strain-hardening behavior of the indented material [26–29]. Identification and quantification of the deformation zone around a nanoindentation imprint is of major importance as the shape of the out-of-plane displacement zone is the actual contact area between the tip and the sample. Sinked-in patterns decrease and pile-up patterns increase the calculated contact area. These deviations in the surface deformation mode influence the quantitative analysis of the contact pressure (as hardness). If piling-up or sinking-in are not considered appropriately during micro- and nanoindentation hardness tests, significant errors may occur when extracting hardness values from the experimental data [30,31]. Creep deformation during nanoindentation testing has an effect on pile-up, which leads to erroneous assessment of the sample properties. Fischer-Cripps noted this behaviour, for cases where the measured modulus of elasticity was found much lower than expected [32]. For identical sample, Rar et al. noted that when allowed to creep for a long testing time, a higher value of pile-up/sink-in was revealed indicating a transition from an initial elastic sink-in deformation to a plastic pile-up deformation [33].

In Figure 2, the normalised pile-up/sink-in height h_c/h_m is plotted vs. displacement (a) and the H/E ratio (b). Rate-sensitive materials exhibit lower pile-up when compared with rate insensitive materials (due to strain hardening) [34]. This is in line with the fact that when h_c/h_m approaches unity for low H/E , the respective deformation is intimately dominated by pile-up (Figure 2d–g) [35,36]. However, when h_c/h_m approaches zero for higher H/E , this corresponds mainly to elastic deformation (dominated by sink-in) [37]. Higher stresses are related with higher H/E (hard materials); increased stress concentrations are developed towards the tip, whereas for low H/E (soft materials), the stresses are found lower and are distributed homogeneously at the cross-section of the material [38,39]. H/E is an index of resistance to wear; high H/E is indicative of the increased wear resistance in a range of materials [39,40]: ceramic, metallic and polymeric. In Figure 2, alter of H/E slope denotes the strengthening of composites with incorporation of 0.5% CNTs, whereas this ratio decreases with incorporation of 3 and 5% CNTs in the PVB matrix. Lower deviation of H/E values for 5% CNTs in

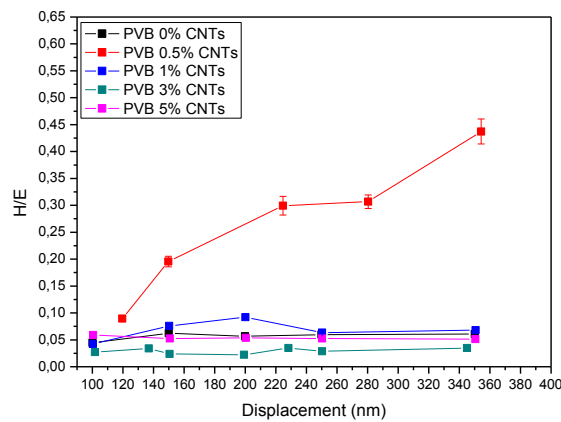
the PVB matrix (PVBC5.0) implies good dispersion in the matrix, leading to almost stable behavior at resistance to wear (~100 to 350 nm displacement range). We can also observe in Figure 2b that while for the pure PVB, h_c/h_m is independent of the normalized hardness H/E , the addition of CNTs leads to a decrease of h_c/h_m for increasing H/E values; this is attributed to the switch from pile-up to sink-in deformation behaviour, after the addition of CNTs.



(a)



(b)



(c)

Figure 2. Cont.

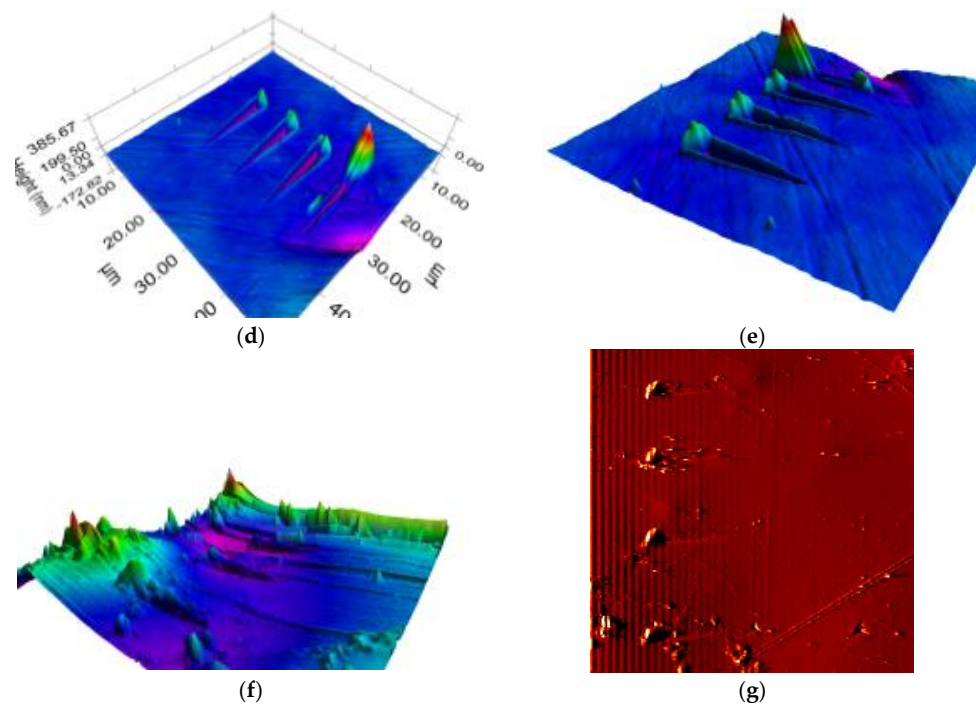


Figure 2. (a) Normalised pile-up/sink-in height h_c/h_m plotted vs. displacement and (b) normalized hardness H/E , for the PVB samples with CNTs, namely PVB 0%, PVB 0.5%, PVB 1%, PVB 2% and PVB 5%. Additionally, the ratio of hardness/elastic modulus (H/E) vs. displacement is plotted (c). Representative SPM images of scratches in PVB ($50 \mu\text{m} \times 50 \mu\text{m}$) (d,e) and PVBC5.0 ($50 \mu\text{m} \times 50 \mu\text{m}$) (f,g) are presented [15].

3.2. MWCNTs/Polydimethylsiloxane-Based Coatings

In Figure 3, H/E and H^3/E^2 ratios are depicted for the PDMS samples with CNTs, namely PDMS 0%, PDMS 0.05%, PDMS 0.1% and PDMS 0.2%, while representative SPM images of scratches in PDMS ($50 \mu\text{m} \times 50 \mu\text{m}$) (d–g) are presented. While H/E ratio has been previously addressed to rank materials as an index of their wear resistance [33–35], H^3/E^2 ratio implies that the amount of elasticity is exhibited by a coating; i.e., high (low) H^3/E^2 values correspond to an elastic (plastic) behavior of the coating [41–43]. In Figure 3, it is noted that the surface of the coating exhibits different results from the bulk of the sample, revealing switch in deformation mechanisms (denoted with dashed lines); the values for depths up to $500 \mu\text{m}$ are verified from previous researches [44]. Furthermore, the H^3/E^2 ratio revealed a similar trend: in principle, plain PDMS presented the greater elastic behavior compared with the rest of the composite samples, with alter of behavior at depths greater than 1600 nm . Moving deeper in the structure of the coating (after 1600 nm), the values for the H/E and H^3/E^2 ratios increase, mainly indicating that addition of 0.1% MWCNTs in PDMS results in enhanced elasticity.

The existence of MWCNTs, both homogeneously dispersed and in a large percentage hinders the scratch of the surface. PDMS 0.1% reveals the lowest coefficient of friction (CoF, μ - Figure 4). An overall evaluation of the results obtained by the scratch tests concludes that low percentage of MWCNTs (0.05%) and the addition of the larger percentage of MWCNTs (0.2%) led to higher values of CoF compared to PDMS 0%; for the case of 0.1% addition, the lowest CoF is evidenced. This high resistance to wear combined with the elastoplastic deformation indicates a change in the structure of the bulk material.

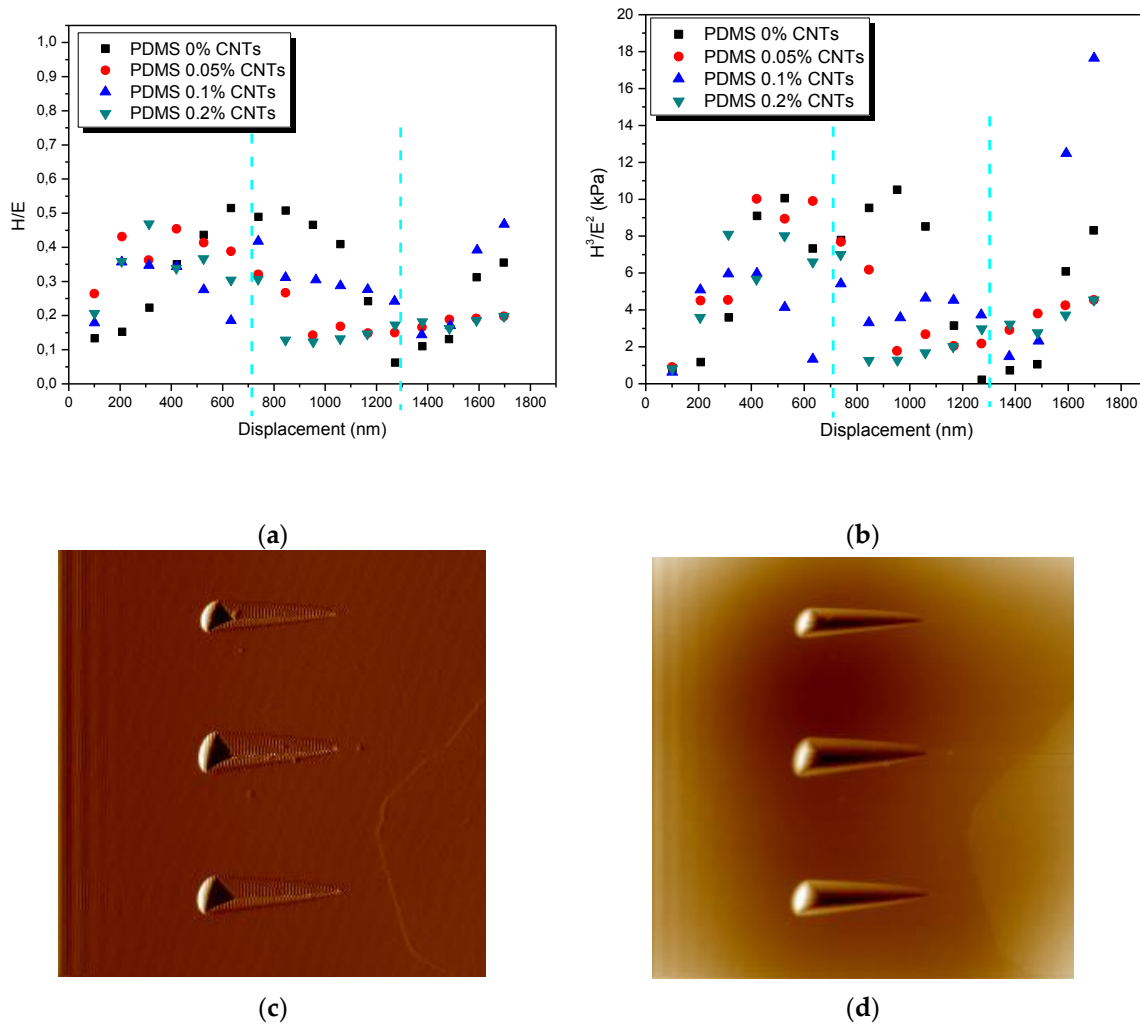


Figure 3. (a) H/E and (b) H^3/E^2 ratios as a function of indentation depth for the PDMS samples with CNTs, namely PDMS 0%, PDMS 0.05%, PDMS 0.1% and PDMS 0.2%. Representative SPM images of scratches in PDMS ($50 \mu\text{m} \times 50 \mu\text{m}$) (c,d) are presented.

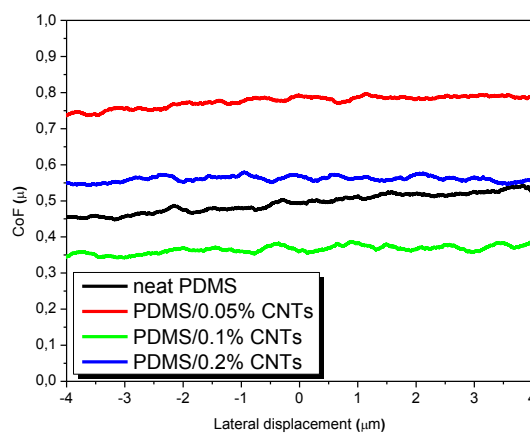


Figure 4. Coefficient of friction (CoF) through nanoscratch testing of the samples PDMS 0% (neat), PDMS 0.05%, PDMS 0.1% and PDMS 0.2%.

3.3. Vertically Aligned CNT Forest Array

Carbon nanotube based architectures have increased the scientific interest owing to their exceptional performance rendering them promising candidates for advanced industrial applications in the nanotechnology field. Despite individual CNTs being considered as one of the most known strong materials, much less is known about other CNT forms, such as CNT arrays, in terms of their mechanical performance. The resistance to nanoscratch of VA-MWCNT forests was investigated; the synthesized VA-MWCNTs forests consisted of well-aligned MWCNTs (Figure 5). Cycle indentation load-depth curve was applied and hysteresis loops were observed in the indenter loading-unloading cycle due to the local stress distribution. Hardness (as resistance to applied load [45]) and modulus mapping, at 200 nm of displacement for a grid of $70 \mu\text{m}^2$ was conducted; through trajectory, the resistance is clearly divided in 2 regions, namely the MWCNT probing and the in-between area MWCNT-MWCNT interface [46]. The CoF (Figure 5) deviates to values below 0.3; scanning (probing) of the sample in a cyclic nanoscratch process is performed. Ploughing of the tip during nanoscratch is attributed to a synergistic mechanism (observed as a periodic phenomenon, e.g., noted in red dashed circles) of individual CNT bending, plastic deformation and accumulation of material ahead of the tip.

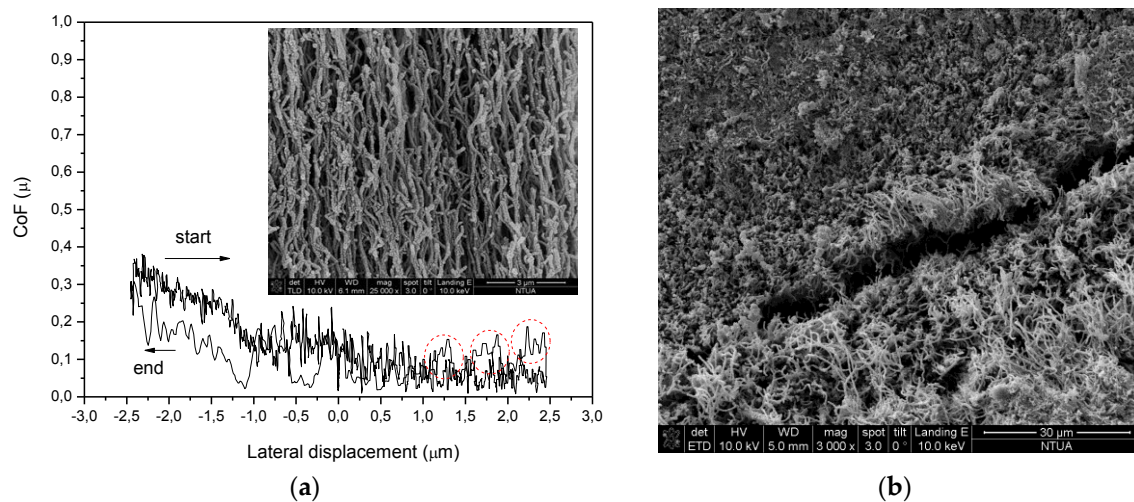


Figure 5. (a) Coefficient of friction (CoF) through nanoscratch testing of vertically aligned CNT forest array (SEM image of the forest as inset) and (b) SEM image of vertically aligned CNT forest array.

4. Conclusions

In this work, three case studies are reported, namely carbon nanotube/polyvinyl butyral composites, MWCNTs/polydimethylsiloxane-based coatings and vertically aligned CNT forest array, of which the friction and resistance to wear/deformation were assessed through nanoindentation/nanoscratch. For the case of carbon nanotube/polyvinyl butyral composites, as CNT concentration is increased, a large increase in the stiffness of the system is evidenced, which results in reduction of the energy dissipated during the experiment. Lower deviation of H/E values for 5% CNTs in the PVB matrix implies good dispersion in the matrix, leading to almost stable behavior at resistance to wear (~ 100 to 350 nm displacement range); also, a transition from pile-up to sink-in deformation behaviour, after the incorporation of CNTs, was evidenced. The friction coefficient is calculated in the 1 to 0.5 range continuously at the initial loading stage of scratching), for 1% CNTs in the PVB matrix and neat PVB matrix. For the case of MWCNTs/polydimethylsiloxane-based coatings, the surface of the coating presents different results from the bulk part of the sample, revealing switch in deformation mechanisms. Plain PDMS presented the greater elastic behavior compared with the rest of the composite samples, with alter of behavior at depths greater than 1600 nm. Moving deeper in the structure of the coating (after 1600 nm), the values for the H/E and H^3/E^2 ratios increase, mainly

indicating that addition of 0.1% MWCNTs in PDMS results in enhanced elasticity. Low percentage of MWCNTs (0.05%) and the addition of the larger percentage of MWCNTs (0.2%) led to higher values of CoF compared to PDMS 0%; for the case of 0.1% addition, the lowest CoF is evidenced. For the case of vertically aligned CNT forest array, CoF deviates to values below 0.3, when applying a scanning (probing) of the sample in a cyclic nanoscratch process. Ploughing of the tip during nanoscratch is attributed to a synergistic mechanism (observed as a periodic phenomenon) of individual CNT bending, plastic deformation and accumulation of material ahead of the tip.

Overall, nanoscratching revealed that there is considerable enhancement of the scratch resistance due to the incorporation of CNTs in a polymer matrix. Addition of CNTs increases the stiffness of the structure, until a concentration threshold beyond which deterioration of the composite begins to occur. For a plain CNT structure (here CNT forest), contact deformation, such as sliding between neighboring nanotubes, results in energy dissipation. Thus, hysteresis can be considered as a material property derived from the local stresses distribution. Through ploughing of the tip, the interfacial contact stresses occur between the inter-CNTs, while CNTs are deformed mainly by local bending; nanoscratching indicated a more plastic rather than elastic response of the CNT forest structure.

Acknowledgments: This work has partially received funding from the European Union's Horizon 2020 research and innovation program MODCOMP under grant agreement No. 685844 and EU FP7 Project FIBRALSPEC under Grant Agreement No. 604248.

Author Contributions: Elias P. Koumoulos and Costas A. Charitidis contributed equally to the following: both conceived and designed the experiments, performed the experiments, analyzed the data, contributed reagents/materials/analysis tools, and wrote the paper.

Conflicts of Interest: The authors declare no conflict of interest.

References

1. Tjong, S.C. Structural and mechanical properties of polymer composites. *Mater. Sci. Eng. R Rep.* **2006**, *53*, 73–197. [[CrossRef](#)]
2. Thostenson, E.T.; Chou, T.W. Processing–structure–multi-functional property relationship in carbon nanotube/epoxy composites. *Carbon* **2006**, *44*, 3022–3029. [[CrossRef](#)]
3. Pegel, S.; Potschke, P.; Villmow, T.; Stoyan, D.; Heinrich, G. Spatial statistics of carbon nanotube polymer composites. *Polymer* **2009**, *5*, 2123–2132. [[CrossRef](#)]
4. Li, W.H.; Chen, X.H.; Chen, C.S.; Xu, L.S.; Yang, Z.; Wang, Y.G. Preparation and shear properties of carbon nanotubes/poly (butyl methacrylate) hybrid material. *Polym. Compos.* **2008**, *29*, 972–977. [[CrossRef](#)]
5. Selmi, A.; Friebel, C.; Doghri, I.; Hassis, H. Prediction of the elastic properties of single walled carbon nanotubes reinforced polymers. *Compos. Sci. Tech.* **2007**, *67*, 2071–2084. [[CrossRef](#)]
6. Kao, C.C.; Young, R.J. Assessment of interface damage during the deformation of carbon nanotubes composites. *J. Mater. Sci.* **2010**, *45*, 1425–1431. [[CrossRef](#)]
7. Bower, C.; Rosen, R.; Han, J.; Zhou, O. Deformation of carbon nanotubes in nanotube polymer composite. *Appl. Phys. Lett.* **1999**, *74*, 3317–3319. [[CrossRef](#)]
8. Li, C.Y.; Wei, T.W. Multiscale modeling of compressive behavior of carbon nanotube polymer composites. *Compos. Sci. Technol.* **2006**, *66*, 2409–2414. [[CrossRef](#)]
9. Giraldo, L.F.; Lopez, B.L.; Bostow, W. Effect of the type of carbon nanotubes on tribological properties of polyamide 6. *Polym. Eng. Sci.* **2009**, *49*, 896–902. [[CrossRef](#)]
10. Wang, C.; Xue, T.; Dong, B.; Wang, Z.; Li, H.L. Polystyrene-acrylonitrile CNTs composites preparation and tribological behavior research. *Wear* **2008**, *265*, 1923–1926. [[CrossRef](#)]
11. Sun, L.Y.; Gibson, R.F.; Gordaninejad, F.; Suher, J. Energy absorption capability of composites: A review. *Compos. Sci. Technol.* **2009**, *69*, 2392–2409. [[CrossRef](#)]
12. Srivastava, V.K. Effect of CNTs on the Wear and Friction Performance of Carbon Fibre Woven Fabric Reinforced Epoxy Resin Composites. *Int. J. Compos. Mater.* **2016**, *6*, 95–99.
13. Zhang, L.C.; Zarudi, I.; Xiao, K.Q. Novel behaviour of friction and wear of epoxy composites reinforced by carbon nanotubes. *Wear* **2006**, *261*, 806–811. [[CrossRef](#)]

14. Zhang, W.; Ma, G.J.; Wu, C.W. Anti-friction, wear-proof and self-lubrication application of carbon nanotubes. *Rev. Adv. Mater. Sci.* **2014**, *36*, 75–88.
15. Charitidis, C.A.; Koumoulos, E.P.; Giorcelli, M.; Musso, S.; Jagadale, P.; Tagliaferro, A. Nanomechanical and tribological properties of carbon nanotube/polyvinyl butyral composites. *Polym. Compos.* **2013**, *34*, 1950–1960. [[CrossRef](#)]
16. Koumoulos, E.P.; Parousis, T.; Trompeta, A.F.A.; Kartsonakis, I.A.; Charitidis, C.A. Investigation of MWCNT addition into poly-dimethylsiloxane-based coatings. *Plast. Rubber Compos.* **2016**, *45*, 106–117. [[CrossRef](#)]
17. Lee, K.-J.; Hsu, M.-H.; Cheng, H.-Z. Effect of Process Parameters of CNT Containing Friction Powder on Flexural Properties and Friction Performance of Organic Brake Friction Materials. *J. Nanomater.* **2014**. [[CrossRef](#)]
18. Li, Y.; Yu, T.; Pui, T.; Chen, P.; Zheng, L.; Liao, K. Fabrication and characterization of recyclable carbon nanotube/polyvinyl butyral composite fiber. *Compos. Sci. Technol.* **2011**, *71*, 1665–1670. [[CrossRef](#)]
19. Kim, K.T.; Jo, W.H. Noncovalent functionalization of multiwalled carbon nanotubes using graft copolymer with naphthalene and its application as a reinforcing filler for poly(styrene-co-acrylonitrile). *J. Polym. Sci. A* **2010**, *48*, 4184–4191. [[CrossRef](#)]
20. Zhuang, G.S.; Sui, G.X.; Sun, Z.S.; Yang, R. Pseudoreinforcement effect of multiwalled carbon nanotubes in epoxy matrix composites. *J. Appl. Polym. Sci.* **2006**, *102*, 3664–3672. [[CrossRef](#)]
21. Ribeiro, R.; Banda, S.; Ounaies, Z.; Ucisik, H.; Usta, M.; Liang, H. A tribological and biomimetic study of PI-CNT composites for cartilage replacement. *J. Mater. Sci.* **2012**, *47*, 649–658. [[CrossRef](#)]
22. Nadler, M.; Werner, J.; Mahrholz, T.; Riedel, U.; Hufenbach, W. Effect of CNT surface functionalisation on the mechanical properties of multi-walled carbon nanotube/epoxy-composites. *Compos. A* **2009**, *40*, 932–937. [[CrossRef](#)]
23. Fiedler, B.; Gojny, F.H.; Wichmann, M.H.G.; Nolte, M.C.M.; Schulte, K. Fundamental aspects of nano-reinforced composites. *Compos. Sci. Technol.* **2006**, *66*, 3115–3125. [[CrossRef](#)]
24. Prashantha, K.; Soulestin, J.; Lacrampe, M.F.; Claes, M.; Dupin, G.; Krawczak, P. Multi-walled carbon nanotube filled polypropylene composites based on masterbatch route: Improvement of dispersion and mechanical properties through PP-g-MA addition. *Express Polym. Lett.* **2008**, *2*, 735–745. [[CrossRef](#)]
25. Koumoulos, E.P.; Charitidis, C.A.; Papageorgiou, D.P.; Papathanasiou, A.G.; Boudouvis, A.G. Nanomechanical and Nanotribological Properties of Hydrophobic Fluorocarbon Dielectric Coating on Tetraethoxysilane for Electrowetting Applications. *Surf. Coat. Technol.* **2012**, *206*, 3823–3831. [[CrossRef](#)]
26. Pharr, G.M.; Oliver, W.C.; Brotzen, F.R. On the generality of the relationship among contact stiffness, contact area, and elastic modulus during indentation. *J. Mater. Res.* **1992**, *7*, 613–617. [[CrossRef](#)]
27. Nix, W.D. Elastic and plastic properties of thin films on substrates: Nanoindentation techniques. *Mater. Sci. Eng. A* **1997**, *234–236*, 37–44. [[CrossRef](#)]
28. Chaudhri, M.M.; Winter, M. The load bearing area of a hardness indentation. *J. Phys. D* **1988**, *21*, 370–374. [[CrossRef](#)]
29. Alcala, J.; Barone, A.C.; Anglada, M. The influence of plastic hardening on surface deformation modes around Vickers and spherical indents. *Acta Mater.* **2000**, *48*, 3451–3464. [[CrossRef](#)]
30. Koumoulos, E.P.; Jagadale, P.; Lorenzi, A.; Tagliaferro, A.; Charitidis, C.A. Evaluation of surface properties of epoxy-nanodiamonds composites. *Compos. B* **2015**, *80*, 27–36. [[CrossRef](#)]
31. Trompeta, A.F.A.; Koumoulos, E.P.; Kartsonakis, I.A.; Charitidis, C.A. Advanced characterization of by-product carbon film obtained by thermal chemical vapor deposition during CNT manufacturing. *Manuf. Rev.* **2017**, *4*, 7. [[CrossRef](#)]
32. Fischer-Cripps, A.C. A simple phenomenological approach to nanoindentation creep. *Mater. Sci. Eng. A* **2004**, *385*, 74–82. [[CrossRef](#)]
33. Rar, A.; Sohn, S.; Oliver, W.C.; Goldsby, D.L.; Tullis, T.E.; Pharr, G.M. *On the Measurement of Creep by Nanoindentation with Continuous Stiffness Techniques*; Materials Research Society: Boston, MA, USA, 2005; pp. 119–124.
34. Cheng, Y.T.; Cheng, C.M. Effects of ‘sinking in’ and ‘piling up’ on estimating the contact area under load in indentation. *Philos. Mag. Lett.* **1998**, *78*, 115–120. [[CrossRef](#)]
35. Hill, R.; Storakers, B.; Zdunek, A.B. A theoretical study of the Brinell hardness test. *Math. Phys. Sci.* **1989**, *423*, 301–330. [[CrossRef](#)]

36. Biwa, S.; Storakers, B. An Analysis of Fully Plastic Brinell Indentation. *Mech. Phys. Sol.* **1995**, *43*, 1303–1333. [[CrossRef](#)]
37. Hertz, H. *Miscellaneous Papers*; Macmillan: London, UK, 1896.
38. Cheng, Y.T.; Cheng, C.M. What is indentation hardness? *Surf. Coat. Technol.* **2000**, *133–134*, 417–424. [[CrossRef](#)]
39. Leyland, A.; Matthews, A. Design criteria for wear-resistant nanostructured and glassy-metal coatings. *Surf. Coat. Technol.* **2004**, *177–178*, 317–324. [[CrossRef](#)]
40. Leyland, A.; Matthews, A. Optimization of Nanostructured Tribological Coatings. In *Nanostructured Coatings*; Springer: New York, NY, USA, 2007; pp. 511–538.
41. Oberle, T.L. Properties influencing wear of metals. *J. Met.* **1951**, *3*, 438–439.
42. Halling, J. Surface films in tribology. *Tribologia* **1982**, *1*, 15–23. [[CrossRef](#)]
43. Leyland, A.; Matthews, A. On the significance of the H/E ratio in wear control: A nanocomposite coating approach to optimised tribological behavior. *Wear* **2000**, *246*, 1–11. [[CrossRef](#)]
44. Koumoulos, E.P.; Jagdale, P.; Kartsonakis, I.A.; Giorcelli, M.; Tagliaferro, A.; Charitidis, C.A. Carbon Nanotube/Polymer Nanocomposites: A Study on Mechanical Integrity through Nanoindentation. *Polym. Compos.* **2014**, *4*, 19. [[CrossRef](#)]
45. Charitidis, C.A.; Koumoulos, E.P.; Dragatogiannis, D.A. Nanotribological Behavior of Carbon Based Thin Films: Friction and Lubricity Mechanisms at the Nanoscale. *Lubricants* **2013**, *1*, 22–47. [[CrossRef](#)]
46. Koumoulos, E.P.; Charitidis, C.A. Surface analysis and mechanical behaviour mapping of vertically aligned CNT forest array through nanoindentation. *Appl. Surf. Sci.* **2017**, *396*, 681–687. [[CrossRef](#)]



© 2017 by the authors. Licensee MDPI, Basel, Switzerland. This article is an open access article distributed under the terms and conditions of the Creative Commons Attribution (CC BY) license (<http://creativecommons.org/licenses/by/4.0/>).